NOTES AND CORRESPONDENCE

A New Metric for Estimating the Influence of Evaporation on Seasonal Precipitation Rates

BRUCE T. ANDERSON AND GUIDO SALVUCCI

Department of Geography and Environment, Boston University, Boston, Massachusetts

ALEX C. RUANE, JOHN O. ROADS, AND MASAO KANAMITSU

Scripps Institution of Oceanography, La Jolla, California

(Manuscript received 21 August 2007, in final form 8 November 2007)

ABSTRACT

The objective of this paper is to introduce a diagnostic metric—termed the *local-convergence ratio*—that can be used to quantify the contribution of evaporation (and transpiration) to the atmospheric hydrologic cycle, and precipitation in particular, over a given region. Previous research into regional moisture (or precipitation) recycling has produced numerous methods for estimating the contributions of "local" (i.e., evaporated) moisture to climatological precipitation and its variations. In general, these metrics quantify the evaporative contribution to the mass of precipitable water within an atmospheric column by comparing the vertically integrated atmospheric fluxes of moisture across a region with the fluxes via evaporation. Here a new metric is proposed, based on the atmospheric moisture tendency equation, which quantifies the evaporative contribution to the *rate* of precipitation by comparing evaporative convergence into the column with large-scale moisture-flux convergence. Using self-consistent, model-derived estimates of the moisture-flux fields and the atmospheric moisture tendency terms, the authors compare estimates of the flux-based moisture-recycling ratio with the newly introduced local-convergence ratio. Differences between the two ratios indicate that they can be considered complementary, but independent, descriptors of the atmospheric hydroclimatology for a given region.

1. Introduction

Traditionally, the regional moisture-recycling ratio (also referred to as the precipitation-recycling ratio), ρ, is defined as the fraction of total precipitation (P) that comprises precipitation of evaporative (or "local") origin (P_l):

$$\rho \equiv \frac{P_l}{P}. \tag{1}$$

As a metric, it is designed to provide information about the contribution of locally derived moisture to the climatological precipitation in a given region. As a diagnostic, it may also provide information about the enhancement/dampening of this precipitation due to land surface–precipitation interactions (Brubaker et al. 1993; Burde and Zangvil 2001a; Bosilovich 2002).

Although fairly straightforward to define in theory, the recycling ratio is more difficult to quantify in practice. There are numerous methods for deriving this ratio; however, they generally are variations of the same set of mathematical equations that depend upon the assumption that the ratio of locally derived precipitation to total precipitation is the same as the ratio of locally derived precipitable water to total precipitable water (w_l and w respectively; Burde and Zangvil 2001a):

$$\rho \equiv \frac{P_l}{P} = \frac{w_l}{w}. \tag{2}$$

Other approaches for estimating moisture recycling involve tracing water from its source region using for-

Corresponding author address: Bruce T. Anderson, Dept. of Geography and Environment, Boston University, 675 Commonwealth Ave., Boston, MA 02215.
E-mail: brucea@bu.edu

DOI: 10.1175/2007JHM968.1

© 2008 American Meteorological Society

ward modeling (Koster et al. 1986; Bosilovich and Schubert 2002), back-trajectory modeling (Dirmeyer and Brubaker 1999), or isotope observations (Wright et al. 2001).

All of these formulations, however, define locally derived precipitation (P_l) as the fraction of water molecules rained out within a given region that originated from the same region via evaporation (as an aside, here and throughout the paper, "evaporation" will be used to represent the conversion of liquid water to water vapor, whether directly or indirectly via transpiration, which is an important source of moisture to the atmosphere in many regions).

Alternatively, locally derived precipitation could be defined as the fraction of total precipitation that is balanced by evaporative contributions to the atmospheric moisture tendency, even if the actual water that precipitates out comes from another region. To see the difference between these two constructs, consider the climatology of a region across which there is a vertically integrated horizontal flux of moisture but in which there is no vertically integrated atmospheric moisture-flux *convergence*; that is, precipitation is balanced by evaporation. In this scenario, precipitable-water-based recycling estimates will indicate that external (or "remote") sources of moisture, advected by the flux field, contribute to the precipitation in the region. To an extent this is correct in that a fraction of the precipitable water that is rained out comes from a nonlocal source. At the same time, the actual precipitation rate for the region is balanced solely by the evaporation rate, regardless of the strength of the horizontal moisture flux. From a hydrologic perspective this influence of evaporation (and moisture-flux convergence) upon the overall precipitation rate seems important to quantify, along with the original source location of the precipitable water itself.

As an example of how these two perspectives can differ, we briefly discuss results from a previous paper examining the summertime atmospheric hydroclimatology over the southwestern United States (Anderson et al. 2004). To calculate the precipitation recycling for this region, we used one traditional method for estimating the recycling ratio (Brubaker et al. 1993), which compares the vertically integrated fluxes of moisture into a region (F_{in}) with the fluxes via evaporation (E) along a parcel trajectory length (L):

$$\rho \equiv \frac{P_l}{P} = \frac{EL}{EL + 2F_{\text{in}}}. \tag{3}$$

From our previous research this recycling ratio was found to be $\rho = 0.23$ for $L = 1000$ km (for $L = 500$ km the recycling ratio is 0.13); alternative estimates based upon the area-averaged fluxes (Eltahir and Bras 1994) give $\rho = 0.26$. The low numbers for the traditional recycling ratios in this region arise because the fluxes via evaporation are small compared with the vertically integrated fluxes of moisture into the region (i.e., EL is small compared with F_{in}). However, results from Anderson et al. (2004) suggest that during summer the rate of vertically integrated moisture-flux *convergence* is actually negative; that is, evaporation balances both precipitation as well as large-scale moisture-flux divergence from the region. In addition, the evaporation rate is over 5 times larger than other sources of moisture convergence into the region (namely, low-level moisture-flux convergence associated with flow from the Gulf of California and Gulf of Mexico). Hence, while the *fluxes* of moisture via evaporation might be small compared to the vertically integrated atmospheric moisture fluxes, the *convergence* of moisture associated with this evaporation is large compared to the moisture-flux convergence. These results suggest the need for a separate metric to quantify this latter relation, which we develop further here.

The principal focus of this paper is to devise such a metric. One key criterion for this metric is that it be based upon estimates of the convergence of moisture (via evaporation and moisture-flux convergence), not simply the fluxes of moisture. Another key criterion is related to the recognition that atmospheric moisture-flux convergence at different levels may be predicated upon sources/sinks from differing regions. For instance, mathematically rigorous precipitation-recycling models based upon the mass continuity equations for moisture (Burde and Zangvil 2001b) rely upon vertically integrated quantities of all variables (moisture and momentum) in order to relate precipitation to precipitable water within a given region [as in Eq. (2)]. However, Bosilovich (2002), using simulated water vapor tracers within general circulation models, has shown that the presumed relation between precipitation and precipitable water may not hold in a vertically integrated sense and that using vertically integrated moisture fluxes masks important processes related to vertical variations in these same quantities. Hence, we argue that the new metric developed here should implicitly account for the fact that there are vertical variations in these hydrologic parameters and not simply rely upon vertically integrated quantities (although some form of vertical integration will eventually be required—see below).

Section 2 provides a derivation of this new metric while section 3 describes the datasets and methods used to estimate it. Section 4 examines results for different climate regimes over the globe. Section 5 provides a

summary and some discussion of further improvements to the metric.

2. Derivation

As a starting point for our derivation of a new metric, consider the vertically integrated moisture tendency equation. Let us define the operator $\{\ldots\}$ as

$$\{\ldots\} = \pi \int_1^0 \ldots d\sigma. \tag{4}$$

Here $\sigma = p(z)/p_s$ and $\pi = p_s/g$ where $p(z)$ is the pressure at a given height (level), p_s is the surface pressure, and g is the gravitational constant. Then the vertically integrated tendency equation for specific humidity (q) becomes

$$\frac{\partial\{q\}}{\partial t} + \nabla \cdot \{\mathbf{u}q\} = E - P. \tag{5}$$

We start with the first term on the left-hand side of the equation. For now we will assume that on climatological time scales (i.e., longer than 10–15 days), the local tendency term ($\partial\{q\}/\partial t$) is near zero (Roads et al. 2002). This assumption is similar to ones employed by most traditional precipitation-recycling estimates as well (Brubaker et al. 1993; Eltahir and Bras 1994; Burde and Zangvil 2001a).

Now consider the second term on the left-hand side of the equation. As discussed in the introduction, it is important to account for the vertical structure of moisture-flux divergence and convergence; hence we do not want to simply use the vertically integrated value of the moisture-flux convergence (i.e., $-\nabla \cdot \{\mathbf{u}q\}$). Instead, we define the *total* moisture-flux convergence (which we will symbolize here as chi, χ, to differentiate it from the vertically integrated net moisture-flux convergence) as the sum of *horizontal* moisture-flux convergence only at levels that have positive values:

$$\chi \equiv \sum_{\sigma} -\nabla_H \cdot \pi\mathbf{u}qd\sigma \;\forall\; (-\nabla_H \cdot \pi\mathbf{u}q > 0), \tag{6}$$

where ∇_H is the two-dimensional divergence operator. It is important to note that convergent levels will be included even if they are not at the same level as condensation and/or precipitation formation because we assume, as done with traditional moisture-recycling estimates, that the atmospheric moisture is well mixed through the column either via convective (i.e., subgrid scale) or large-scale vertical fluxes. Again, this quantity differs from the vertically integrated net moisture-flux convergence, which would represent the sum of moisture-flux convergence at all levels (given by $\Sigma_\sigma - \nabla \cdot \pi\mathbf{u}qd\sigma$).

By analogy, we define the total moisture-flux divergence (δ) as the sum of the horizontal moisture-flux divergence only at levels that have positive values:

$$\delta \equiv \sum_{\sigma} \nabla_H \cdot \pi\mathbf{u}qd\sigma \;\forall\; (\nabla_H \cdot \pi\mathbf{u}q > 0). \tag{7}$$

Since the vertical sum of the vertical moisture-flux divergence term ($(\partial\pi\dot{\sigma}q/\partial\sigma)$) is 0 when integrating through the entire atmospheric column,

$$\chi - \delta = -\nabla \cdot \{\mathbf{u}q\} = P - E. \tag{8}$$

Rearranging gives

$$P + \delta = E + \chi. \tag{9}$$

This balance can be written as

(precipitation + total moisture-flux divergence)

= (evaporation + total moisture-flux convergence).

Hence, while evaporation in and of itself is not a precipitation-producing process (in the same way convection or orographic lifting is), from this equation we see that on climatic time scales (longer than approximately 10 days) evaporation rates can serve to balance precipitation rates (as well as moisture divergence rates). In this sense, evaporation, and metrics derived from evaporation (such as precipitation-recycling ratios and the new local-convergence ratio, discussed below) may provide limited information about the meteorological rainfall-producing *processes* that are acting within a region. However, on a climatological scale they can provide an estimate of the contribution of evaporation to the precipitable water and precipitation rates within a region (even if evaporation itself does not produce the precipitation).

Next, to estimate this contribution of evaporation to the rate of precipitation (as opposed to the amount of precipitable water), we compute the area-average evaporation E (kg m^{-2} s^{-1}) through the bottom of the atmospheric column. Since there can be no vertical moisture flux out of the top of the atmospheric column, this term represents a convergence of moisture into the column (and hence is also referred to as "evaporative convergence"). This evaporative convergence is augmented by total moisture-flux convergence (χ). Some of the moisture supplied by E and χ precipitates out; what does not precipitate out is removed via total moisture divergence, δ. Figure 1 shows a schematic of the hydrologic balance for an atmospheric column given these assumptions.

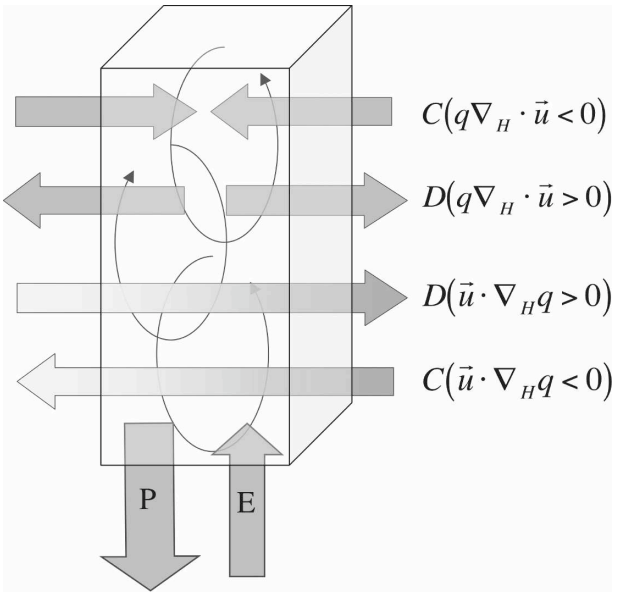

FIG. 1. Schematic of moisture convergence terms used to calculate the local-convergence metric: P—precipitation; E—evaporation; C—levels in which moisture-flux convergence (related to both gradients in winds and moisture) is occurring. Here, $\nabla_H \cdot \pi \mathbf{u} q < 0$, and hence these levels contribute to χ (see text for details); D—levels in which moisture-flux divergence (related to both gradients in winds and moisture) is occurring. Here, $\nabla_H \cdot \pi \mathbf{u} q > 0$, and hence these levels contribute to δ (see text for details). Thin black arrows represent mixing within the column.

Based upon the assumption that the convergent moisture (i.e., as supplied by E and χ) is well mixed, we now assume that the proportion of precipitation balanced by the local convergence of moisture (P_{lc}) and that balanced by moisture-flux convergence from outside the region (P_{fc}) are in the same ratio as the area-averaged evaporative convergence (E) and the total moisture-flux convergence (χ).

Making the assumptions above allows us to write

$$P = P_{\mathrm{lc}} + P_{\mathrm{fc}} = \frac{E}{E+\chi} P + \frac{\chi}{E+\chi} P. \qquad (10)$$

We will then define the "local-convergence ratio," λ, as

$$\lambda \equiv \frac{P_{\mathrm{lc}}}{P} = \frac{E}{E+\chi}. \qquad (11)$$

Although the local-convergence ratio and the recycling ratio have similar forms, here we give them different names in order to highlight that one (the local-convergence ratio) is a convergence-based estimate and one (the precipitation-recycling ratio) is a flux-based estimate. Other important characteristics to note are as follows:

- In this formulation, P_{lc} is not equivalent to E, but is instead some fraction of E, with the remainder of E balancing divergence of moisture from the region (δ), that is, the ratios in Eq. (11) are equal but the numerators and denominators are not the same.
- Because the total moisture-flux convergence, χ, can never be negative (since only convergent levels are included) this version of the local-convergence ratio will always be less than 1 and greater than 0 (except under certain circumstances when climatological evaporation is negative, for instance, during periods of deposition in the high latitudes in winter).
- We reiterate that χ is not the same as net vertically integrated moisture-flux convergence, $-\nabla \cdot \{\mathbf{u}q\}$. If the two were equivalent then $E + \chi = P$ and the local-convergence ratio would simply be the ratio of evaporation to precipitation. In that case, certain regions could have a local-convergence ratio greater than one (e.g., in regions where net vertically integrated moisture-flux convergence is negative and hence $E > P$).

We also want to reemphasize the physical differences between the two ratios. The recycling ratio provides an estimate of the fraction of water molecules rained out within a given region that originated from within the region via evaporation (compared with the fraction supplied via vertically integrated atmospheric moisture fluxes). In this sense, it quantifies the "local" contribution of mass available for precipitation. In contrast, the local-convergence ratio provides an estimate of the fraction of the overall precipitation rate that is balanced by convergence of moisture via evaporation (as compared with the rate of precipitation that is balanced by moisture-flux convergence at various levels in the atmosphere), independent of where the water molecules originated. Hence, it quantifies the "local" contribution to the moisture tendency within a given region that in turn can balance precipitation within the same region.

3. Data and methods

a. Data

For this study, we will use 3 yr of 6-h model forecasts taken from the National Centers for Environmental Prediction–Department of Energy (NCEP–DOE) Reanalysis-2 model. A full description of these model runs is provided in Ruane and Roads (2007a,b). Here we provide a brief overview. To perform these forecasts, the NCEP–DOE Reanalysis-2 model (RII; Kanamitsu et al. 2002) initialized with the NCEP–NCAR Reanalysis-2 data, along with a linear interpolation of weekly-mean sea surface temperature values, was used to produce augmented 6-h forecasts 4 times each day (at 0000, 0600, 1200, and 1800 UTC). This global model uses the

primitive (prognostic) equations for virtual temperature, humidity, surface pressure, and momentum, resolved in the horizontal with spherical harmonics at a triangular truncation of 62 and in the vertical with 28 sigma levels. Output is provided every 3 h on a 192×94 Gaussian grid, with pixels approximately 1.9° across. The RII utilizes the simplified Arakawa–Schubert (Pan and Wu 1995) convection scheme. In addition, the land surface evolution is driven by the Oregon State University Land Surface Model (Pan and Mahrt 1987), which consists of two vertical layers in the top 2 m of soil. The RII then adjusts the soil moisture as dictated by the biases computed when the model precipitation is compared to observed precipitation over 5-day pentads (Lu et al. 2005). The integrations from this model were carried out for the Coordinated Enhanced Observing Period (CEOP, 2002–04; Lawford et al. 2006). The precipitation and atmospheric hydrology diagnostics from these model runs have been evaluated in Ruane and Roads (2007a,b). Here we will utilize the relevant global T62 gridpoint data pertaining to the atmospheric hydrologic cycle (see below). In addition, we will analyze prognostic and diagnostic model data at individual grid points that contain the 41 CEOP Model Output Location Time Series (MOLTS) stations (Lawford et al. 2006).

b. Methods

Some of the atmospheric hydrologic quantities needed for this analysis are standard output from most numerical model systems; however, others require post-processing of the data before they are suitable for use in the study. Here we will describe the various terms used for the two different metrics.

1) PRECIPITATION RECYCLING

For the precipitation-recycling method, because we will be using point-source data for specific locations (i.e., CEOP–MOLTS stations), we will use the method of Brubaker et al. (1993). As given in Eq. (3), this method compares the fluxes of moisture into a region (F_{in}) with the fluxes via evaporation (E) along a parcel trajectory length (L):

$$\rho \equiv \frac{P_l}{P} = \frac{EL}{EL + 2F_{\text{in}}}.$$

A schematic of the hydrologic fluxes within a particular region is given in Fig. 4 of Trenberth (1999). The model outputs both the time-average evaporation rate (E) for the 3-h integration period, as well as the instantaneous vertically integrated moisture-flux components (i.e., zonal and meridional) at the end of the integration period. For the parcel trajectory length scale, we need to adopt a value for L. As in Trenberth (1999), we select $L = 500$ km throughout this study. When multiplied by L we will refer to the evaporation term (EL) as the "evaporative flux" (to differentiate it from evaporation, which has units of kg m^{-1} s^{-1}). To arrive at an estimate of F_{in}, we simply find the magnitude of the vertically integrated moisture-flux vector using the two component moisture-flux vectors.

It should be noted that a similar version of this metric comes from Eltahir and Bras (1994), in which the precipitation recycling for a single grid cell is given by the evaporative fluxes within the grid cell and the respective integrated moisture-flux components passing across the sides of the grid cell. While these two forms are not equivalent, results are qualitatively the same when using the Eltahir and Bras (1994) ratio as opposed to the Brubaker et al. (1993) ratio.

Limitations with both of these methods have been pointed out in Burde and Zangvil (2001a), particularly with regard to assumptions about the orientation and characteristics of the moisture-flux field; however, given point-source data for specific locations (whether from a model or observations) these methods represent one of the few ways to estimate the precipitation recycling without resorting to tracer methods.

2) LOCAL-CONVERGENCE RATIO

For the local-convergence ratio [Eq. (11)] we need to estimate

$$\lambda \equiv \frac{P_{\text{lc}}}{P} = \frac{E}{E + \chi}.$$

As mentioned, the model outputs the time-average evaporation rate (E) for the 3-h integration period, which we will use here. When used in the local-convergence ratio, we will refer to this term as "evaporation" as well as "evaporative convergence" to emphasize that it has units of kg m^{-2} s^{-1} and produces a convergence of moisture into the column.

The estimation for the total moisture-flux convergence term, χ, is not directly computed by the model and hence must be derived as a residual from other hydrologic terms. However, in order to integrate the moisture tendency equation at each model time step (approximately every 20 min), the model does calculate the three-dimensional moisture-flux divergence term at each sigma level, DQ(σ):

$$\text{DQ}(\sigma) = \boldsymbol{\nabla} \cdot \pi \mathbf{u} q + \frac{\partial \pi \dot{\sigma} q}{\partial \sigma}. \tag{12}$$

Therefore we have modified the code of the model such that the instantaneous value of this term at the end of

the 3-h integration period becomes part of the data output stream.

We then use this full three-dimensional moisture-flux divergence term at each level to estimate the *horizontal* moisture-flux divergence term at the given level (assuming that the vertical component acts in conjunction with turbulent diffusion to mix moisture between levels). To do this we first archive the mass-weighted vertical moisture fluxes ($\pi\dot{\sigma}q$) at each level (which like the three-dimensional moisture-flux divergence values are instantaneous values provided by the model as part of the output stream at the end of each 3-h integration). We then derive the vertical moisture-flux divergence term, VDQ(σ), by taking the vertical derivative of $\pi\dot{\sigma}q$:

$$\mathrm{VDQ}(\sigma) = \frac{\partial}{\partial \sigma}(\pi\dot{\sigma}q). \tag{13}$$

Subtracting this from the full three-dimensional moisture-flux divergence term gives just the horizontal moisture-flux divergence term for the given level, HDQ(σ):

$$\mathrm{HDQ}(\sigma) = \mathrm{DQ}(\sigma) - \mathrm{VDQ}(\sigma). \tag{14}$$

For the local-convergence ratio, we want an estimate of total moisture-flux convergence (χ), which we define as the sum of horizontal moisture-flux convergence only at levels that have positive values. Using the nomenclature above, this gives

$$\chi \equiv \sum_{\sigma} -\mathrm{HDQ}(\sigma)d\sigma \;\forall\; (-\mathrm{HDQ}(\sigma) > 0). \tag{15}$$

Again, it is important to note that in order for the original balance to hold [Eq. (9)], we need to take a time average over a relatively long time period in order to make the assumption that the local tendency term is zero. A sensitivity analysis indicates that values of χ are quantitatively similar (within 25%) when using averaging periods ranging from 20 to 90 days (not shown). Because evaporation is insensitive to time averaging past the synoptic time scale (values are within 10% of one another for averaging periods ranging from 5 to 90 days), the resulting estimates of the local-convergence ratio, λ, also show good agreement (within 15%) for averaging periods ranging from 20 to 90 days (not shown). As such, to derive λ for this paper we will adopt a 30-day averaging period to estimate the climatological profiles for HDQ(σ) before we perform the vertical summation to arrive at χ. We also perform a similar 30-day time average for all other quantities (i.e., *E, EL,* and F_{in}). For seasonal-mean values of the two ratios (i.e., ρ and λ), we then take the average of these 30-day mean hydrologic quantities across the 3 months within the season before computing the respective ratios via Eqs. (3) and (11) (results are quantitatively the same if the two ratios are first computed for each month and then averaged over the 3-month period).

4. Results

Figure 2 shows maps of a traditional measure of the recycling ratio (Brubaker et al. 1993) along with the local-convergence ratio for the December–February period and the June–August period, using the 30-day time-average data described above. The first thing to note is the differing scales of the two ratios. The recycling ratio tends to lie between values of 0 and 0.5, although in certain locations it can become larger than 0.5. In contrast, the local-convergence ratio tends to lie between 0.2 and 0.8. This difference reflects the fact that the sizes of the evaporative fluxes relative to the vertically integrated atmospheric moisture fluxes are generally smaller than the sizes of the evaporative convergence relative to the total moisture-flux convergence (see Figs. 4, 5).

Examining first the precipitation-recycling ratios, one striking feature is the very narrow, zonal bands stretching across Africa, Australia, and South America. These are particularly prevalent in boreal winter; however, they are also present during boreal summer. These are an artifact of using monthly-mean flux fields combined with the simple area-average diagnostics; in these regions tropical winds are weak and hence vertically integrated moisture fluxes are small, resulting in fairly large recycling ratios. Similar features are also found in longer-term climatological values. For instance, Fig. 8 from Trenberth (1999) shows similar zonal bands during the December–February period across all three regions. In addition, both maps show similar zonal patterns extending across India, Southeast Asia, and Central America. It should be noted that back-trajectory analysis, which accounts for both submonthly time-scale interactions between transient fields as well as variations in flow across regions, effectively removes these zonal bands, although spatial patterns elsewhere are similar (Dirmeyer and Brubaker 2007).

Outside of the zonal-banding regions, the recycling ratio indicates lower values in mid- to high-latitudes during hemispheric winter and higher values during hemispheric summer (throughout the manuscript, hemispheric summer refers to boreal summer for the Northern Hemisphere and austral summer for the Southern Hemisphere; similar designations apply for hemispheric winter). These results again are in agreement with traditional estimates taken from longer-term climatological values (Trenberth 1999) and more so-

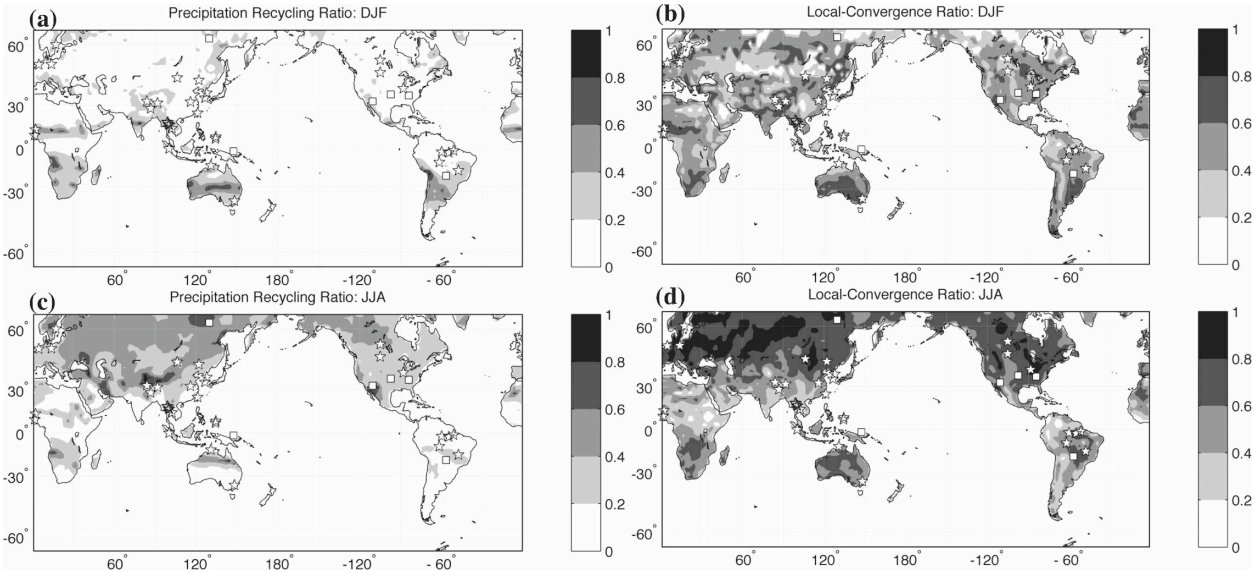

FIG. 2. (a) Seasonal-mean precipitation-recycling ratio for December–February (DJF) derived from Brubaker et al. (1993). Estimates based on 30-day averages of evaporation and vertically integrated moisture fluxes for the respective months. Length scale, L, is 500 km. Data are derived from 3-h integrations of the Reanalyis-2 atmospheric model (see text for details). White stars represent Reanalysis-2 atmospheric model grid points corresponding to the 41 CEOP stations. White squares represent six CEOP stations analyzed in this paper. (b) Same as in (a), but for seasonal-mean local-convergence ratio derived from Eq. (11). Estimates based on 30-day averages of evaporation and total moisture-flux convergence, χ, for the respective months (see text for details). (c) Seasonal-mean precipitation-recycling ratio for June–August (JJA) derived from Brubaker et al. (1993). (d) Same as in (c), but for seasonal-mean local-convergence ratio derived from Eq. (11).

phisticated back-trajectory analyses (Dirmeyer and Brubaker 2007).

In comparison to the Brubaker et al. (1993) recycling ratio estimates, the local-convergence ratio does not show the strong zonal structures in the low latitudes. However, the local-convergence ratio does contain regional variations throughout the mid- and high latitudes during both seasons. As with the recycling ratio, the local-convergence ratio shows lower values during hemispheric winter and higher values during hemispheric summer. At the same time, the values for the local-convergence ratio are systematically higher than those for the recycling ratio, particularly during hemispheric winter (see Fig. 3), suggesting that local evaporation may have a more prominent role in contributing to seasonal precipitation rates than is implied by recycling ratios (this discrepancy between λ and ρ is true both when calculating ρ using simple area-average diagnostics or more sophisticated back-trajectory analyses, which also generally fall between 4% and 10% during this time; see Fig. 5 from Dirmeyer and Brubaker 2007).

Because it is difficult to distinguish regional characteristics of the seasonal evolution within these maps, Fig. 3 shows the seasonal evolution of the local-convergence ratio and precipitation-recycling ratio for three specific sites in North America—the Atmospheric Radiation Measurement Program (ARM) site in the southern Great Plains (characteristic of a dry midlatitude climate), Oak Ridge in Tennessee (characteristic of a moist continental climate), and Mount Bigelow in Arizona (characteristic of a North American monsoon climate). In addition, three other sites are selected—the ARM site in Manus (characteristic of tropical ocean regions), the Pantanal site in Brazil (characteristic of a South American monsoon climate), and a site in Siberia (characteristic of a tundra climate). We had wanted to select an Indian or East Asian monsoon site. Unfortunately no CEOP station locations are found in the core of the Indian monsoon region. In addition, the three Southeast Asian sites (two Chao Phraya River sites and one site in northeast Thailand) all lie along the artificially high band of precipitation recycling found during boreal winter (as determined by the dissimilarity between the recycling ratio along this band and the values directly to the north and south of this band, which tend to be much lower). Hence instead we chose a South American site, which can be considered to have a monsoonlike precipitation evolution (see Vera et al. 2006).

Figure 4 shows, for each of the six stations, the relative sizes of the "local" and "remote" (or external) terms that go into the two metrics. For the recycling

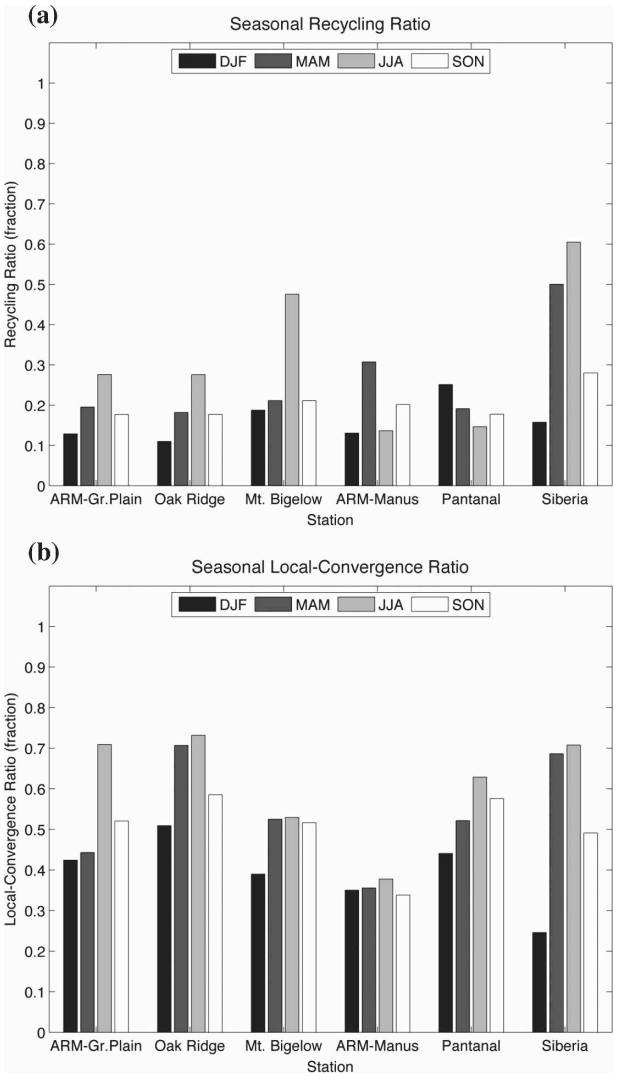

FIG. 3. (a) Seasonal-mean precipitation-recycling ratios derived from Brubaker et al. (1993) for six CEOP–MOLTS sites; see Fig. 2 for station locations. Estimates based on 30-day averages of evaporation and vertically integrated moisture fluxes for the respective months. Length scale, L, is 500 km. Data derived from 3-h integrations of the Reanalyis-2 atmospheric model (see text for details). (b) Seasonal-mean local-convergence ratio derived from Eq. (11). Estimates based on 30-day averages of evaporation and total moisture-flux convergence, χ, for the respective months (see text for details). Data derived from 3-h integrations of the Reanalyis-2 atmospheric model.

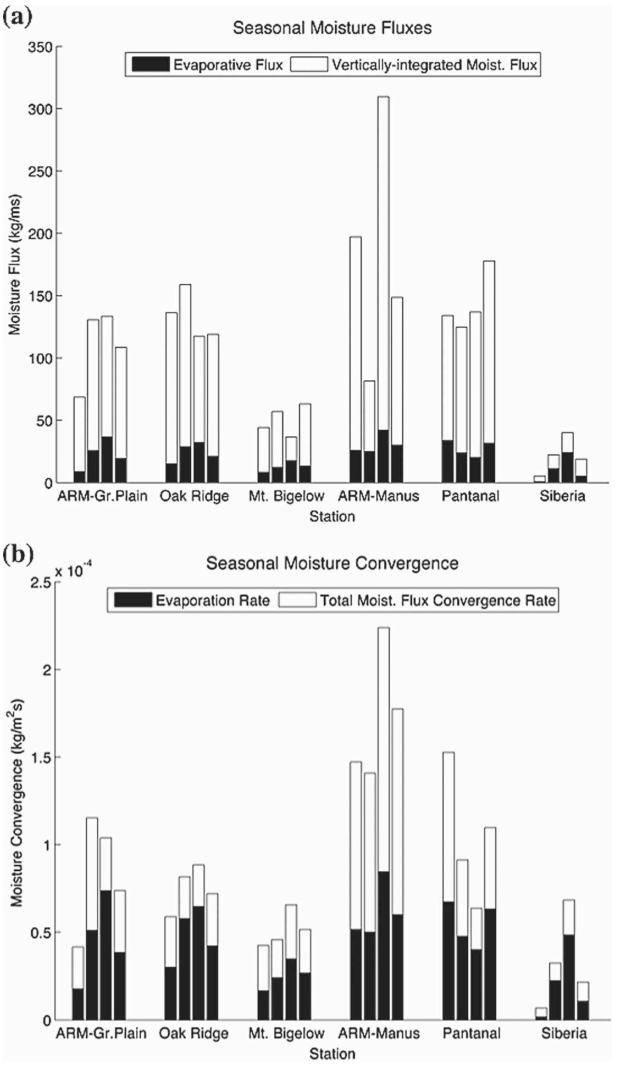

FIG. 4. (a) Seasonal-mean evaporative fluxes and vertically integrated moisture fluxes for six CEOP–MOLTS sites; see Fig. 2 for station locations. Four bars represent same four seasons as in Fig. 3. Evaporative fluxes estimated using length scale, L, of 500 km. Data derived from 3-h integrations of the Reanalyis-2 atmospheric model (see text for details). (b) Seasonal-mean evaporation and total moisture-flux convergence, χ (see text for details). Data derived from 3-h integrations of the Reanalyis-2 atmospheric model.

ratio, these comprise the evaporative flux, EL, and the vertically integrated moisture vapor flux, F_{in}, respectively. For the local-convergence ratio, these comprise evaporation, E, and the total moisture-flux convergence, χ, defined above.

Starting with the Southern Great Plains site, the low recycling ratios throughout the year are related to the relatively large vertically integrated fluxes of moisture emanating from the Gulf of Mexico that pass over this region (Fig. 4a; Schmitz and Mullen 1996). In comparison, the local-convergence metric tends to be 2–3 times larger than the recycling ratio because of the relatively small total moisture-flux convergence term (Fig. 4b). Over the course of the year, the local-convergence metric tends to follow the same evolution as the recycling ratio, with minimum values during boreal winter and maximum values during boreal summer. One exception arises in boreal spring (March–May) when the local-

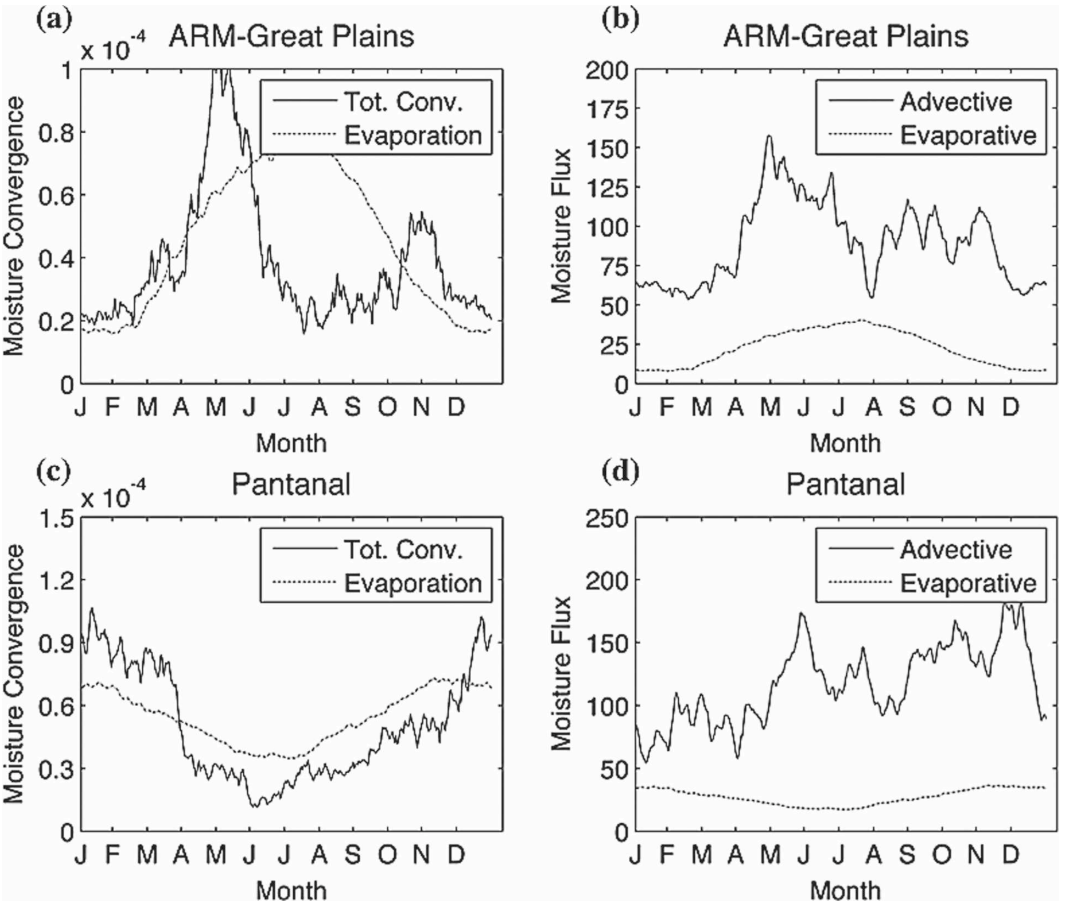

FIG. 5. (a) Climatological 30-day running mean of evaporation (dashed line) and total moisture-flux convergence, χ (solid line), for ARM Southern Great Plains site. Thirty-day running means calculated as the box average centered on the given day; climatological values represent the average over the three simulation years. Data derived from 3-h integrations of the Reanalyis-2 atmospheric model. Units are kg m^{-2} s^{-1}. (b) Same as (a), but for evaporative fluxes (dashed line) and vertically integrated moisture fluxes (solid line). Evaporative fluxes estimated using length scale, L, of 500 km. Units are kg m^{-1} s^{-1}. (c), (d) Same as (a), (b), but for the Pantanal, Brazil, site.

convergence ratio is suppressed compared with its value during summer and fall. During this time, χ increases significantly compared with the values during the rest of the year (Fig. 4b); hence the local-convergence rate remains fairly low. In contrast, F_{in}, which also peaks in spring, remains high through summer and fall (see Fig. 5); hence the precipitation-recycling ratio tends to follow the evaporative flux term, EL, which has maximum values during spring and summer (Fig. 4a).

At Oak Ridge, the recycling ratio is again minimum during winter when the evaporative fluxes are a minimum and the vertically integrated moisture fluxes are a maximum (Fig. 4a). During spring, F_{in} remains high; however, an increase in EL in turn leads to an increase in the recycling ratio. During summer and fall F_{in} decreases such that the recycling ratio remains high. Interestingly, this seasonal evolution for the recycling ratio is almost identical to the ARM Great Plains site, albeit for different reasons (see Fig. 4a). The local-convergence ratio, however, shows differing seasonal evolutions between the two sites. As at the ARM Southern Great Plains site, the local-convergence ratio is a minimum during winter. However, during spring, the value of χ decreases while the value of E increases, resulting in a much higher local-convergence ratio over Oak Ridge than over the ARM Great Plains site (this difference is in contrast to the Oak Ridge/ARM Southern Great Plains recycling ratios during spring, which show very similar values). The values of the local-convergence ratio remain high during summer, then decrease in fall as χ begins to increase and E begins to decrease.

The Mount Bigelow site in Arizona also shows differences in the seasonal evolutions of the precipitation-recycling and local-convergence ratios. For the precipi-

tation-recycling ratio, there are low values throughout most of the year except during the summer months when the monsoon is active. The summertime increase in the recycling ratio is related to a decrease in F_{in} (Fig. 4a). During this period, this region sits near the center of the monsoon circulation; hence horizontal moisture fluxes weaken considerably (Higgins et al. 1997; Anderson and Roads 2001), resulting in higher values for the precipitation-recycling ratio. Similar maximums are found throughout this region during this period (Fig. 2). [Methods for calculating precipitation-recycling given inhomogeneous, nonparallel flux fields can partially account for this seasonal change in circulation patterns, although even these cannot account for a reversal of flow within a given region (Burde and Zangvil 2001b).] In contrast, the value of the local-convergence metric during summer is similar to its value during spring and fall. While Fig. 4b indicates that during summer the evaporation is higher than in spring, there is also an increase in χ during this time. Hence the relatively low local-convergence ratio suggests that moisture-flux convergence remains an important contributor to summertime precipitation, in contrast to the results derived from the recycling ratio.

In the tropical region of Manus, the moisture-recycling ratio appears to follow the evolution of the vertically integrated moisture-flux term, F_{in}. During boreal winter and summer, F_{in} is at a maximum (Fig. 4a); hence the precipitation-recycling values are at a minimum. Conversely, during boreal spring and fall values of F_{in} are generally smaller and hence the precipitation-recycling values are at a maximum. In this region, F_{in} (and hence the precipitation-recycling term) is following the seasonal migration of the trade wind/ITCZ regime, with lulls during the equinoxes and maximums during the two solstices. In contrast, the local-convergence ratio indicates fairly constant values through the year, even during high-evaporation periods when χ also increases (Fig. 4b), suggesting fairly uniform evaporative contributions to precipitation throughout the year. Other low-latitude oceanic sites in Fig. 2 have similar seasonal evolutions (not shown).

At the Pantanal site, the precipitation-recycling ratio shows a maximum in austral summer (December–February) and a minimum in austral winter (June–August). The austral winter minimum is related to a minimum in evaporative fluxes, EL, during this time (Fig. 4a). The austral summer maximum occurs because EL is at a maximum, while F_{in} is a minimum, particularly in January and February (see Fig. 5d). The seasonal evolution of the two flux terms produces a seasonal evolution in the precipitation-recycling ratio, which is opposite that of the local-convergence ratio. For instance, the recycling ratio shows a minimum in austral winter while the local-convergence ratio shows a maximum (Fig. 3b). During this wintertime period, both evaporation and total moisture-flux convergence, χ, are at a minimum. However, the more dramatic decrease in χ subsequently leads to a large increase in the local-convergence ratio. In addition, while the recycling ratio shows a maximum during the austral summer monsoon season, the local-convergence ratio shows a distinct minimum, related to an increase in χ during this time (see Fig. 5c).

At Siberia, as well as other high-latitude continental regions (not shown), the two ratios show similar seasonal evolution. Here F_{in} appears to have a similar evolution as χ. Because the evaporative terms are proportional to one another, the ratios also tend to follow one another and indicate minimums in winter and maximums in summer.

To further investigate the seasonal evolution of these two ratios and their respective components, the climatological 30-day mean convergence terms (evaporation and total moisture-flux convergence) along with the climatological 30-day mean flux terms (evaporative and vertically integrated moisture fluxes) are plotted for the Southern Great Plains site and the Pantanal, Brazil, site (Fig. 5). Here 30-day running means are calculated as the box average centered on a given day; the climatological values represent the average on the given day based upon the values for each of the three simulation years. For the Southern Great Plains site, there is a significant maximum in χ centered on March. Profiles of horizontal moisture-flux convergence during this time indicate that this enhancement is associated with convergence at lower levels (not shown), most likely related to the known intensification of the Great Plains low-level jet (Higgins 1996). During late summer and early fall, however, χ falls off and the period is dominated by large values of E, suggesting evaporation plays an important role in balancing summertime precipitation rates in this region. The F_{in} values also show a maximum during spring. However, unlike χ, these remain relatively high through summer and into fall. Hence, the precipitation-recycling ratio does not show the same dramatic summertime increase that the local-convergence ratio does (Figs. 3a,b), suggesting that a large fraction of the precipitable water that does rain out during this time originates from outside the region.

The difference in these two terms is also apparent over a monsoon region such as Pantanal, Brazil. Here, the total moisture-flux convergence term, χ, shows a maximum centered on January with a decrease in April and minimum values lasting through October. In contrast, during the summertime monsoon season (Decem-

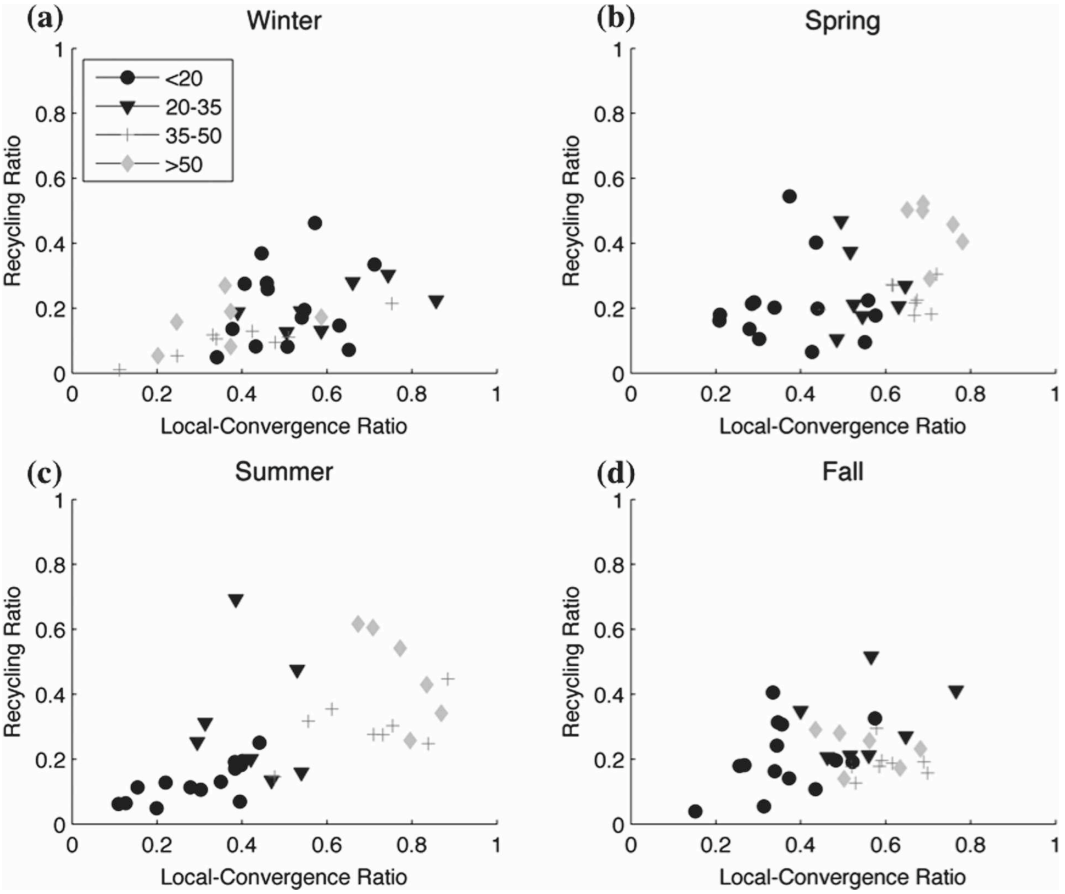

FIG. 6. (a) Seasonal-mean wintertime precipitation-recycling ratios derived from Brubaker et al. (1993) for all 41 CEOP–MOLTS sites plotted against the seasonal-mean wintertime local-convergence ratio derived from Eq. (11). Wintertime season determined by hemisphere—Northern Hemisphere: DJF; Southern Hemisphere: JJA. Precipitation-recycling estimates based on 30-day averages of evaporative and vertically integrated moisture fluxes for the respective months. Length scale, L, is 500 km. Local-convergence ratios based on 30-day averages of evaporation and total moisture-flux convergence, χ, for the respective months (see text for details). Data derived from 3-h integrations of the Reanalyis-2 atmospheric model (see text for details). Different symbols represent the latitude band for the given station. (b) Same as in (a), but for spring. (c) Same as in (a), but for summer. (d) Same as in (a), but for fall.

ber–February; Grimm 2003), the vertically integrated moisture-flux term, F_{in}, shows a distinct minimum when the region sits within the center of the monsoon-induced circulation (Vera et al. 2006). In addition, the F_{in} values begin to increase in April–May as the region comes under the influence of the poleward edge of the northward-moving monsoon circulation. Values of F_{in} remain high through November–December, and then collapse at the same time χ starts to increase. Hence the seasonal evolution of the precipitation-recycling ratio shows a marked (austral) summertime peak while the local-convergence ratio indicates a summertime minimum (Figs. 3a,b). This summertime minimum in the local-convergence ratio suggests that the monsoon rains in this region are balanced predominantly by an increase in the total moisture-flux convergence term, as opposed to local evaporation of soil moisture, in agreement with previous analyses of the hydrologic cycle here (Lenters and Cook 1995; Li and Fu 2004). However, the precipitation-recycling ratio indicates that a relatively high fraction of the precipitable water that does rain out originates from within the region (as compared with other times of year).

Above we examined the similarities and differences between the two ratios, and their respective components, at specific sites to see what terms contributed to each. To see how the local-convergence and precipitation-recycling ratios compare at all sites, Fig. 6 plots the two ratios against one another for each hemispheric season (i.e., Southern Hemisphere summer is designat-

ed as December–February and Northern Hemisphere summer is designated June–August). Here we also differentiate the sites based upon their latitude. Overall, it appears that there is most agreement between the two ratios during hemispheric summer. The values tend to fall along a quasi-linear line indicating that regions with higher local-convergence ratios also have higher precipitation-recycling ratios during this season. However, this generalization does not apply at all latitudes. For instance, in the subtropics (20°–35°) there does not appear to be any relation between the local-convergence ratio and the precipitation-recycling ratio. In addition, at high latitudes (>50°), there actually appears to be an inverse relation between the two ratios.

The largest differences between the two ratios tend to occur in spring. Here the spread is fairly large. Regions with low local-convergence values tend to have low precipitation-recycling ratios; however, the converse is not necessarily true. In addition, for higher values of the local-convergence ratio, there are broad ranges of recycling ratios (and vice versa). Also, none of the latitudinal regions show any apparent relation between the two ratios.

During fall and winter, the values are relatively dispersed, as during spring, and there does not seem to be the same quasi-linear relationship as during summer. For the same value of the precipitation-recycling metric, there is a broad range of values for the local-convergence ratio and, when accounting for the smaller dynamic range of the recycling ratio, the same holds true in reverse.

More generally, this figure highlights the fact that the precipitation-recycling ratio and the local-convergence ratio are *not* redundant metrics and therefore may be considered two complementary, but independent, descriptors of the regional atmospheric hydrologic cycle for a given region.

5. Summary

We have proposed a new tendency-based metric for estimating the influence of evaporation upon the atmospheric hydrologic cycle, and precipitation in particular, over a given region. By accounting for water vapor convergence into a region, as opposed to the fluxes of moisture through a region, this diagnostic metric relates climatological precipitation rates to the hydrologic balances that support the rainfall itself.

Results using self-consistent, model-derived estimates of the moisture-flux fields, as well as the atmospheric moisture tendency terms, suggest that flux-based precipitation-recycling ratios and the newly introduced local-convergence ratios show similarities in certain regions (e.g., high-latitude regions) and times of year (predominantly summertime). However, in other regions the two metrics differ in important ways. For instance, over tropical regions the local-convergence ratio contains less seasonality than the recycling ratio, which is driven by seasonal shifts in the positioning of the vertically integrated moisture fluxes associated with the trade wind/ITCZ regime. In addition, during the rainy seasons over monsoon regions (Pantanal, Brazil, and Mount Bigelow, Arizona) the local-convergence ratios tend to decrease as large-scale moisture-flux convergence associated with the monsoon circulations intensifies; in contrast, the precipitation-recycling ratios increase as vertically integrated moisture fluxes within the monsoon circulations weaken. Similarly, over the Great Plains region in spring the local-convergence ratio is relatively small as low-level moisture-flux convergence plays a predominant role in balancing precipitation; in summer, however, the convergence associated with these moisture fluxes decreases and the local-convergence ratio increases dramatically. In contrast, the precipitation-recycling ratio indicates only a small increase from spring to summer as the vertically integrated moisture fluxes remain fairly large throughout.

Here we suggest that the newly developed local-convergence ratio can aid in analyses of the climatological contribution of evaporation and moisture-flux convergence to regional rainfall rates. In the future, we will examine how variability in this index compares with variability in precipitation itself. These studies in turn should provide information about the enhancement/dampening of the precipitation rate due to land surface/precipitation interactions and hence about the role local and remote sources of moisture play in balancing low-frequency (interseasonal and longer) precipitation variability. However, because of the limited time span of the dataset used here (only 3 yr), it is not feasible to investigate this issue presently. Another limitation of the local-convergence metric derived here, as well as of traditional precipitation-recycling metrics in general, is that they are based upon monthly- and/or seasonal-mean variables. This issue has been addressed by Dominguez et al. (2006) for the recycling ratio, and they find that incorporating daily time-scale variations increases the estimates of precipitation recycling by 10%–30% (at least for the continental United States during summer). Given these significant differences, in the future we will derive a version of the local-convergence metric that can be used for only those time periods (i.e., days) in which precipitation is occurring. This new derivation should allow us to estimate the contribution of local evaporation (as well as total mois-

ture-flux convergence and moisture tendency) to precipitation rates during rainfall events themselves.

REFERENCES

Anderson, B. T., and J. O. Roads, 2001: Summertime moisture divergence over the southwestern US and northwestern Mexico. *Geophys. Res. Lett.,* **28,** 1973–1976.

——, H. Kanamaru, and J. O. Roads, 2004: The summertime atmospheric hydrologic cycle over the southwestern United States. *J. Hydrometeor.,* **5,** 679–692.

Bosilovich, M. G., 2002: On the vertical distribution of local and remote sources for precipitation. *Meteor. Atmos. Phys.,* **80,** 31–41.

——, and S. D. Schubert, 2002: Water vapor tracers as diagnostics of the regional hydrologic cycle. *J. Hydrometeor.,* **3,** 149–165.

Brubaker, K. L., D. Entekhabi, and P. S. Eagleson, 1993: Estimation of continental precipitation recycling. *J. Climate,* **6,** 1077–1089.

Burde, G. I., and A. Zangvil, 2001a: The estimation of regional precipitation recycling. Part I: Review of recycling models. *J. Climate,* **14,** 2497–2508.

——, and ——, 2001b: The estimation of regional precipitation recycling. Part II: A new recycling model. *J. Climate,* **14,** 2497–2508.

Dirmeyer, P. A., and K. L. Brubaker, 1999: Contrasting evaporative moisture sources during the drought of 1988 and the flood of 1993. *J. Geophys. Res.,* **104,** 19 383–19 397.

——, and ——, 2007: Characterization of the global hydrologic cycle from a back-trajectory analysis of atmospheric water vapor. *J. Hydrometeor.,* **8,** 20–37.

Dominguez, F., P. Kumar, X.-Z. Liang, and M. Ting, 2006: Impact of atmospheric moisture storage on precipitation recycling. *J. Climate,* **19,** 1513–1530.

Eltahir, E. A. B., and L. B. Bras, 1994: Precipitation recycling in the Amazon basin. *Quart. J. Roy. Meteor. Soc.,* **120,** 861–880.

Grimm, A. M., 2003: The El Niño impact on the summer monsoon in Brazil: Regional processes versus remote influences. *J. Climate,* **16,** 263–280.

Higgins, R. W., 1996: The moisture budget of the central United States in spring as evaluated in the NCEP/NCAR and the NASA/DAO reanalyses. *Mon. Wea. Rev.,* **124,** 939–963.

——, Y. Yao, and X. L. Wang, 1997: Influence of the North American monsoon system on the U.S. summer precipitation regime. *J. Climate,* **10,** 2600–2622.

Kanamitsu, M., W. Ebisuzaki, J. Woollen, S. K. Yang, J. J. Hnilo, M. Fiorino, and G. L. Potter, 2002: NCEP–DOE AMIP-II Reanalysis (R-2). *Bull. Amer. Meteor. Soc.,* **83,** 1631–1643.

Koster, R., J. Jouzel, R. Souzzo, G. Russel, D. Rind, and P. S. Eagleson, 1986: Global sources of precipitation as determined by the NASA/GISS GCM. *Geophys. Res. Lett.,* **13,** 121–124.

Lawford, R., and Coauthors, 2006: U.S. contributions to the CEOP. *Bull. Amer. Meteor. Soc.,* **87,** 927–939.

Lenters, J. D., and K. H. Cook, 1995: Simulation and diagnosis of the regional summertime precipitation climatology of South America. *J. Climate,* **8,** 2988–3005.

Li, W., and R. Fu, 2004: Transition of the large-scale atmospheric and land surface conditions from the dry to the wet season over Amazonia as diagnosed by the ECMWF re-analysis. *J. Climate,* **17,** 2637–2651.

Lu, C.-H., M. Kanamitsu, J. O. Roads, W. Ebisuzaki, K. E. Mitchell, and D. Lohmann, 2005: Evaluation of soil moisture in the NCEP–NCAR and NCEP–DOE global reanalyses. *J. Hydrometeor.,* **6,** 391–408.

Pan, H.-L., and L. Mahrt, 1987: Interaction between soil hydrology and boundary layer developments. *Bound.-Layer Meteor.,* **38,** 185–202.

——, and W.-S. Wu, 1995: Implementing a mass flux convection parameterization package for the NMC Medium-Range Forecast Model. NMC Office Note 409, 40 pp. [Available from NCEP/EMC 5200 Auth Road, Camp Springs, MD 20746.]

Roads, J., M. Kanamitsu, and R. Stewart, 2002: CSE water and energy budgets in the NCEP–DOE Reanalysis II. *J. Hydrometeor.,* **3,** 227–248.

Ruane, A. C., and J. O. Roads, 2007a: The diurnal cycle of water and energy over the continental United States from three reanalyses. *J. Meteor. Soc. Japan,* **85A,** 117–143.

——, and ——, 2007b: 6-hour to 1-year variance of five global precipitation sets. *Earth Interactions,* **11.** [Available online at http://EarthInteractions.org.]

Schmitz, J. T., and S. L. Mullen, 1996: Water vapor transport associated with the summertime North American monsoon as depicted by ECMWF analyses. *J. Climate,* **9,** 1621–1634.

Trenberth, K. E., 1999: Atmospheric moisture recycling: Role of advection and local evaporation. *J. Climate,* **12,** 1368–1381.

Vera, C. S., and Coauthors, 2006: Toward a unified view of the American monsoon systems. *J. Climate,* **19,** 4977–5000.

Wright, W. E., A. Long, A. C. Comrie, S. W. Leavitt, T. Cavazos, and C. Eastoe, 2001: Monsoonal moisture sources revealed using temperature, precipitation, and precipitation stable isotope timeseries. *Geophys. Res. Lett.,* **28,** 787–790.

Copyright of Journal of Hydrometeorology is the property of American Meteorological Society and its content may not be copied or emailed to multiple sites or posted to a listserv without the copyright holder's express written permission. However, users may print, download, or email articles for individual use.